

Thermoresponsive/Low-Fouling Zwitterionic Hydrogel for Controlled Drug Release

Renchang Zeng, Shouping Xu, Jiang Cheng, Zhiqi Cai, Pihui Pi, Xiufang Wen

College of Chemistry and Chemical Engineering, South China University of Technology, Guangzhou 510640, People's Republic of China

Correspondence to: S. Xu (E-mail: cespxu@scut.edu.cn)

ABSTRACT: A controlled/ living free-radical polymerization technique was introduced to prepared a homogeneous poly(*N*-isopropylacrylamide)-*g*-poly(sulfobetaine methacrylate) hydrogel (RG) possessing a highly porous architecture via two steps. Compared to a poly(*N*-isopropylacrylamide)-*co*-poly(sulfobetaine methacrylate) hydrogel (CG) prepared by conventional radical polymerization, RG exhibited a much faster shrinking rate (it lost over 72% of the water in 15 min) in response to the temperature changes. The release behaviors of tetracycline hydrochloride (TCHC) of the hydrogels indicated the TCHC release from the RG could be prolonged to 48 h at 37°C; this was much longer than that for CG (5 h at 37°C). Bovine serum albumin (BSA) was chosen as the model protein to examine the low-fouling properties of the RG. The BSA adsorption data showed that improved antifouling properties could be achieved by the RG at both 25 and 37°C. © 2013 Wiley Periodicals, Inc. *J. Appl. Polym. Sci.* **2014**, *131*, 39816.

KEYWORDS: biomaterials; drug-delivery systems; stimuli-sensitive polymers; swelling

Received 7 May 2013; accepted 4 August 2013

DOI: 10.1002/app.39816

INTRODUCTION

Stimuli-responsive hydrogels are three-dimensional polymeric networks with the ability to respond to external stimuli, such as temperature, pH, and ionic strength.^{1–3} The poly(*N*-isopropylacrylamide) (PNIPAM) hydrogel is one of the most popularly investigated temperature-sensitive hydrogels, and it has been widely explored for drug delivery, mass separations, and tissue engineering.^{4–6} Since the fast thermoresponsive PNIPAM hydrogel was first developed by Yoshida et al.,¹ it has received great attention because of its huge potential for sustained drug release over a longer period. PNIPAM hydrogels can shrink rapidly in response to temperature changes; this makes the hydrogel network compact. A tight structure leads to an increase in the high-density region in the surface of the hydrogel; this was proposed to be responsible for the sustained release of the drug.⁷ However, when used as a drug-release device, the PNIPAM hydrogel probably suffers from protein fouling on the surface, and the adsorbed protein would block its responsive functional groups and make the gel fail to respond rapidly to shifts in temperature. Therefore, the exploitation of new types of fast thermoresponsive and low-fouling hydrogels is critical for its application in drug release.

One effective strategies for keeping the rapid thermoresponsive properties of a gel is the fabrication of the grafted hydrogel by the introduction of graft chains in the polymeric network.⁸ This

is because the graft chains in the network can provide water-releasing channels and allow the water inside the gel to diffuse out quickly when the temperature changes.⁹ Many reports have demonstrated the preparation of the rapidly shrinking hydrogel bearing grafted side chains. However, little attention has been paid to the improvement of the protein resistance of the hydrogel. For example, Yoshida et al.¹ and Okano et al.⁸ reported a grafted PNIPAM hydrogel with hydrophilic graft chains; it exhibited a rapid deswelling rate, but the antifouling properties of the gel were not investigated. Kim et al.¹⁰ synthesized a rapid temperature-/pH-responsive alginate-*g*-PNIPAM hydrogel with a porous structure, which showed repeatable shrinking–swelling behaviors. However, the hydrophobicity of the hydrogel surface increased when the temperature changed, and this was unfavorable for the resistance to protein adsorption. Liu and coworkers^{11,12} prepared two kinds of grafted *N*-isopropylacrylamide (NIPAM) hydrogels by the introduction of PNIPAM and poly(acrylic acid) as graft chains. Despite the acceleration of the shrinking rate in the hydrogel, both of them still showed a low protein-resistance ability because of the hydrophobic aggregation of the network at 37°C.

Poly(sulfobetaine methacrylate) (PSBMA) is a biocompatible and hydrophilic polyzwitterionic polymer, which can form a hydration layer between the PSBMA surface and protein molecule via electrostatic interaction and hydrogen bonding.^{13,14} The

hydration layer on the PSBMA surface is supposed to be highly resistant to protein adsorption. For instance, Zhang et al.¹³ prepared a series of uniform PSBMA brushes on the gold surface; it was found that fibrinogen adsorption on the *N*-(3-sulfo-propyl)-*N*-(methacryloxyethyl)-*N,N'*-dimethyl ammonium betaine (SBMA)-grafted surface was less than 0.3 ng/cm². Chiang et al.¹⁵ grafted PSBMA onto the surface of a poly(vinylidene fluoride) membrane via atom transfer radical polymerization; this PSBMA-grafted membrane was found to effectively resist albumin adsorption during filtration. If the PSBMA chains are introduced as graft chains in the NIPAM network, the antifouling properties of the grafted PNIPAM hydrogel may be enhanced. Thus, it is possible to synthesize thermoresponsive hydrogels with protein-resistance properties with PSBMA as the graft chains. As far as we know, reports on the study of the thermoresponsive and low-fouling hydrogels are rare.

Reversible addition–fragmentation chain transfer (RAFT) polymerization is a controlled/ living free-radical polymerization technique used to prepare well-defined polymers in both aqueous and nonaqueous media.^{16,17} Some researchers have reported the synthesis of grafted hydrogels via RAFT polymerization in nonaqueous media.^{11,12} However, a nonaqueous reaction medium, such as 1,4-dioxane, is unsuitable for carrying out the reaction for preparing the hydrophilic graft chains, and the organic solvent is unfriendly to the environment.

Herein, we introduce an aqueous RAFT polymerization technique for synthesizing grafted poly(*N*-isopropylacrylamide)-*g*-poly(sulfobetaine methacrylate) hydrogel (RG) with water-soluble 2-(2-carboxyethylsulfanylthiocarbonyl sulfanyl) propionic acid (TTC) as a chain-transfer agent via two steps. In this study, the morphological characterization, shrinking rate, antifouling properties and drug-release kinetics of the hydrogel were investigated and compared with a hydrogel prepared by the conventional free-radical polymerization method.

EXPERIMENTAL

Materials

NIPAM, *N,N'*-methylene bisacrylamide (MMBA), ammonium persulfate (APS), bovine serum albumin (BSA), and Coomassie Brilliant Blue G-250 were purchased from Aladdin Chemicals (Shanghai, China). Phosphate-buffered saline (PBS) and tetracycline hydrochloride (TCHC) were obtained from AMRESCO. SBMA was further purified by dissolution and recrystallization in ethanol. TTC was synthesized by a previously published method.¹⁸

Synthesis of the Grafted RGs

SBMA (0.5 g, 1.81 mmol), APS (0.0054 g, 0.024 mmol), TTC (0.0065 g, 0.024 mmol), and distilled water (4.0 mL) were added to a polymerization tube with magnetic stirring. After three freeze–pump–thaw cycles, the polymerization tube was sealed *in vacuo*, SBMA polymeric chains (PSBMA) were synthesized at 40°C for 24 h under stirring. Then, a solution of NIPAM (1.5 g, 13.3 mmol), PSBMA (0.5 g, 1.81 mmol), APS (0.0054 g, 0.024 mmol), and MMBA (0.08 g, 0.52 mmol) in 8 mL of deionized water was added to a polymerization tube. After the tube was sealed under nitrogen, the reaction was conducted at 35°C for 24 h to produce the grafted RG. For com-

parison, the poly(*N*-isopropylacrylamide)-*co*-poly(sulfobetaine methacrylate) hydrogel (CG) was prepared by conventional radical polymerization under the same conditions. Briefly, SBMA (0.5 g, 1.81 mmol), NIPAM (1.5 g, 13.3 mmol), and MMBA (0.08 g, 0.52 mmol) were dissolved in 12 mL of deionized water, and then APS (0.0054 g, 0.024 mmol) was added to the solution to initiate the polymerization at 35°C, and the reaction was performed under a nitrogen atmosphere for 24 h. These two kinds of hydrogels were immersed in deionized water for 48 h to remove the unreacted chemicals. Both of them were cut into small discs (10 mm in diameter and 3 mm in thickness) for further testing.

Characterization of Hydrogels

Fourier transform infrared (FTIR) spectroscopy with a Bruker Vector 33 spectrophotometer was used to evaluate the chemical compositions of the hydrogels in the range 4000–500 cm⁻¹.

The exact morphologies of RG and CG were visualized by scanning electron microscopy (SEM; HITACHI S-3700N). These hydrogels were freeze-dried to get rid of water and were coated with gold before SEM observation.

The swelling ratio (SR) of the hydrogel was determined as follows:

$$SR = (m_s - m_d) / m_d$$

where m_s is the mass of the swollen hydrogel at a certain temperature and m_d is the mass of the dry hydrogel.

We measured the shrinking behaviors of the hydrogel by transferring the equilibrated swollen hydrogel at room temperature to deionized water at 45°C and recording the weight of the hydrogel during collapse at different times. The water retention (WR) was computed as follows:

$$WR = (m_t - m_d) / m_s$$

where m_t is the weight of the hydrogel at a certain times during shrinking.

In Vitro Release of TCHC by the Hydrogels

The freeze-dried hydrogels were immersed in a TCHC aqueous solution (7.0 mg/mL, 10 mL) at room temperature for 48 h to reach equilibrium; after equilibrium was reached, the excess water on the surfaces was wiped off, and these gels were placed at room temperature for 24 h and dried *in vacuo* for 48 h.

The *in vitro* drug-release studies were carried out at 25 and 37°C, respectively. Dried drug-entrapped RG (or CG) was transferred to 50 mL of deionized water. At given time intervals, 5.0 mL of drug-release solution was withdrawn for concentration measurement by a UV spectrophotometer (UV-2450, Shimadzu) at 357 nm and replaced with 5.0 mL of fresh distilled water simultaneously. All of the drug-release tests were performed in triplicate. The release kinetics were determined as follows:

$$\text{Release kinetics} = M_t / M_0 \times 100\%$$

where M_t is the amount of drug in the release medium at a fixed time and M_0 is the amount of drug before release.

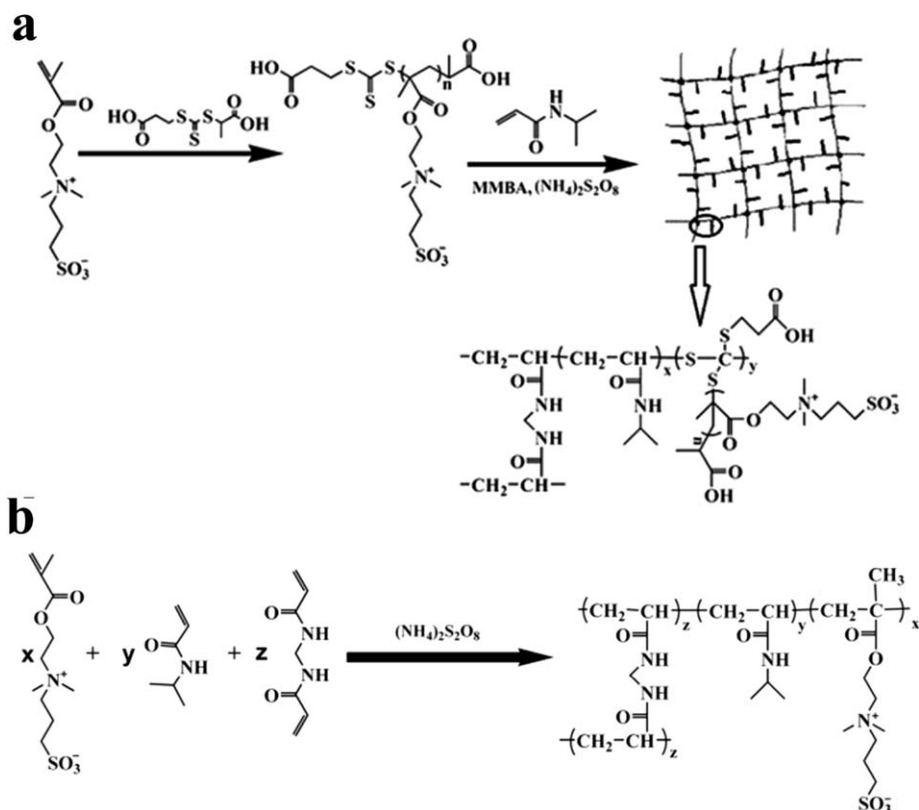


Figure 1. Process for synthesizing the (a) RG by RAFT polymerization and (b) CG by free-radical copolymerization.

In Vitro Protein Adsorption Test

A Bio-Rad protein assay was used to evaluate the protein adsorption of the zwitterionic hydrogels with BSA as a model protein. Hydrogel disks (10 mm in diameter and 3 mm in thickness) were soaked in PBS (0.01M, 20 mL) for 30 min. Then the disks were transferred into BSA solutions (1.0 mg/mL, 10 mL), which were prepared with PBS solutions for 24 h at 25 and 37°C, respectively. The hydrogels were removed from BSA solutions, and this was followed by the addition of the coloring agent (Coomassie Brilliant Blue G-250) into the solutions. The protein concentration of the solutions was determined with a UV spectrometer (UV-2450, Shimadzu) to measure the absorption at 595 nm. The calibration curve was preset by the measurement of the solutions with various protein concentrations. The protein adsorption ($\mu\text{g}/\text{cm}^2$) of the hydrogels could be calculated by the following equation:

$$\text{Protein adsorption} = \frac{(C_0 - C_t) \times V}{A}$$

where C_0 and C_t are the BSA concentrations before and after the hydrogel was soaked in BSA solution ($\mu\text{g}/\text{mL}$), V is the volume of the solution, and A is the effective surface area of the hydrogel (cm^2).

RESULTS AND DISCUSSION

Preparation of Grafted Hydrogel

In this study, RG was prepared by aqueous RAFT polymerization via two steps [as illustrated in Figure 1(a)]. PSBMA bearing

a thiocarbonylthio [$-\text{C}(=\text{S})\text{S}-\text{R}$] end was first synthesized, and then it worked as a macromolecular chain-transfer reagent to react with NIPAM to form the grafted hydrogel in the presence of MMBA. On the contrary, CG was synthesized by the free-radical copolymerization of SBMA and NIPAM in one step. As shown in Figure 1(b), SBMA and NIPAM were initiated to form the CG with MMBA as a crosslinker.

The FTIR spectra for the pure PNIPAM hydrogel, SBMA hydrogel, CG, and RG are presented in Figure 2. In the spectrum of the pure PNIPAM hydrogel [Figure 1(a)], the intensities of the band at 1542 and 3071 cm^{-1} were ascribed to the bending and stretching of the N—H bond in NIPAM,¹⁹ and the characteristic peak at 2876 cm^{-1} due to the stretching of the C—H bond in $-\text{CH}(\text{CH}_3)_2$ was observed. These peaks are also found in spectra b and c; this indicated the presence of NIPAM in both the CG and RG. In addition, spectra b and c displayed characteristic bands at 1040 and 1730 cm^{-1} , which were also seen in the spectrum of the SBMA hydrogel [Figure 1(d)]. These absorption bands resulted from the stretching vibration of $-\text{SO}_3^-$ and the ester carbonyl ($\text{C}=\text{O}$) existing in the structure of SBMA,^{16,20} this suggested the successful incorporation of SBMA into the gel network of the CG and RG. Moreover, the intensity of the band at 1460 cm^{-1} was assigned to the bending vibrations of the C—H bond in $-\text{CH}(\text{CH}_3)_2$ and $-(\text{CH}_2)_2$, and the broad band in the range from 1100 to 1350 cm^{-1} was attributed to the stretching of C—N in NIPAM and the C—O—C structure in SBMA.²⁰

The surface morphologies of the RG and CG are shown in Figure 3(a). The CG exhibited highly heterogeneous crosslinking

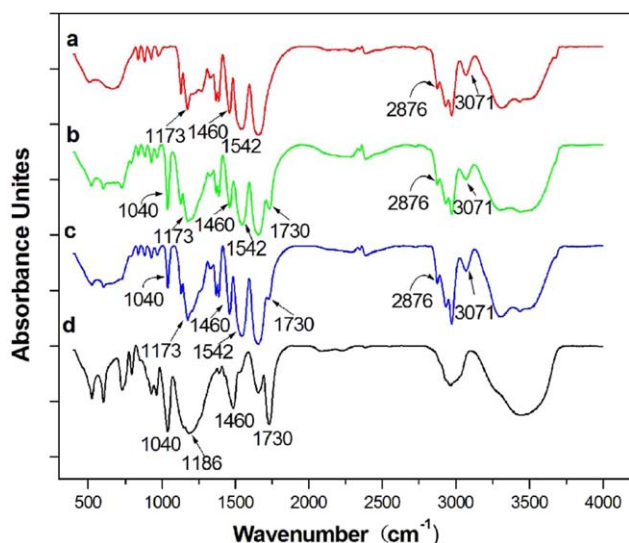


Figure 2. FTIR spectra of the (a) PNIPAM hydrogel, (b) CG, (c) RG, and (d) PSBMA hydrogel. [Color figure can be viewed in the online issue, which is available at wileyonlinelibrary.com.]

and an uneven mass distribution. This was because gel formation by free-radical copolymerization proceeded in a highly nonideal way; this probably resulted in the formation of cycles

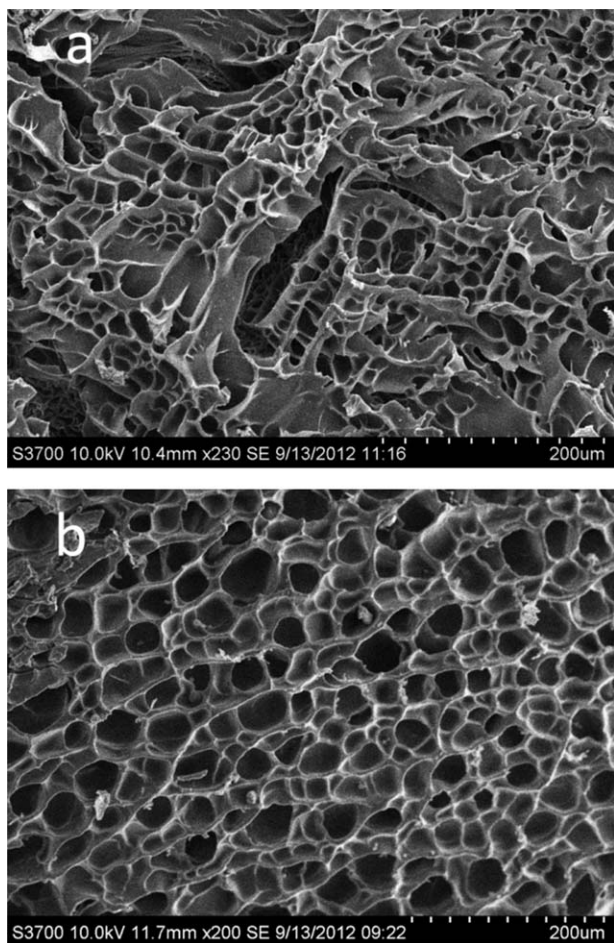


Figure 3. SEM images of (a) CG and (b) RG.

or intermolecular crosslinks.¹¹ In contrast, as shown in Figure 3(b), RG showed a homogeneous architecture with uniform pore diameters ranging from 20 to 40 μm ; this probably resulted from the well-controlled properties of RAFT polymerization. The homogeneous porous microstructure in the RG matrix was supposed to allow water to diffuse out more easily than in the CG during the shrinking process. To test the shrinking kinetics of the RG, the swollen RG was transferred into 45°C distilled water in comparison with the CG.

Shrinking Kinetics

The shrinking behaviors of the porous RG and CG are illustrated in Figure 4(a), from which we observed that the porous RG showed a much faster shrinking rate than the CG. For instance, the RG lost over 72% water in 15 min, whereas CG just lost 25% water in 15 min. This was because the uncontrolled intermolecular binding and crosslink between PNIPAM and PSBMA weakened the thermoresponsive functional groups of PNIPAM in the process of synthesizing CG; this resulted in a much slower shrinking rate.^{8,12} In comparison with CG, few intermolecular crosslinks happened in the RAFT polymerization, and a homogeneous network structure with the PSBMA-grafted chains was formed during gelation. In the shrinking process, the hydrophilic grafted chains diffused out to restrict the strong hydrophobic aggregation of the NIPAM backbone and offered water-releasing channels simultaneously.¹¹ Thus, the water inside the gel could be squeezed out quickly.

In addition, we conducted the shrinking–swelling experiments of the RG and CG by changing the temperature between 25 and 45°C in the cycle of 48 h. As illustrated in Figure 4(a), the equilibrium SR of the CG decreased from 3.7 to 2.8 after two shrinking–swelling cycles, whereas the swelling–shrinking process of the RG was repeatable with little SR change. This suggested that the RG had stable thermosensitive properties in response to temperature change. The structural stability of the RG gives it great potential application in the design of drug-release system. The decrease in the equilibrium SR of the CG may have been due to the reduced pore size¹⁰ caused by the unstable network structure.

Drug-Release Studies

The possibility of the drug releasing from the RG was investigated with hydrophilic TCHC as a model drug at 25 and 37°C. As comparison, the drug release from CG was examined at the same temperatures. As presented in Figure 5(a), we observed that both CG and RG exhibited a burst release of TCHC within the initial 2 h at 25°C. The release amounts of drug in the first 2 h were 54% for the CG and 37% for the RG, respectively. Then the release rate gradually decreased with less TCHC released at the equal time interval, and the release times of the CG and RG were 6 and 12 h, respectively. During the first stage, large amounts of TCHC were loaded in the surface of the hydrogel, and the burst release was mainly driven by the concentration gradient between the hydrogel surface and the surrounding medium. In the following stage, the swelling rate was the main driving force for drug release. The slowing down of the release rate was ascribed to the reduced TCHC concentration and the slow swelling of the hydrogel. However, because of

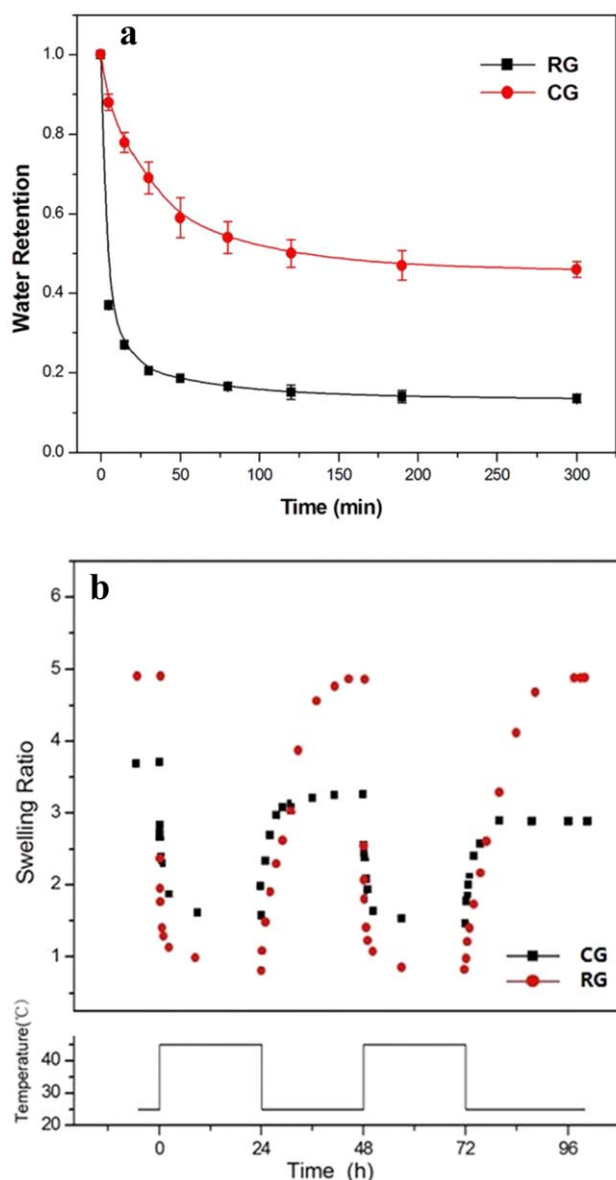


Figure 4. (a) Shrinking kinetics of the conventional and RAFT hydrogels via the transfer of equilibrated swollen hydrogels at room temperature to deionized water at 45°C. (b) Reversible shrinking–swelling behaviors of RG and CG between 25 and 45°C. [Color figure can be viewed in the online issue, which is available at wileyonlinelibrary.com.]

the low shrinkage of the CG and RG at 25°C, the regional density of the surface was so low that the gel could reach the swollen equilibrium in a relatively short time. The swollen state of the gel allowed TCHC molecules to diffuse out into the release medium easily. Thus, most of the TCHC was released from the RG and CG within 12 h; this made both of them incapable of achieving sustained release for a long time.

Figure 5(a) also shows the cumulative release of the TCHC from the CG at 37°C. The TCHC release time of the CG at 37°C was 5 h; this was shorter than that at 25°C. It was suggested that the CG showed a faster release rate at 37°C. This result may have been caused by the following two reasons: (1)

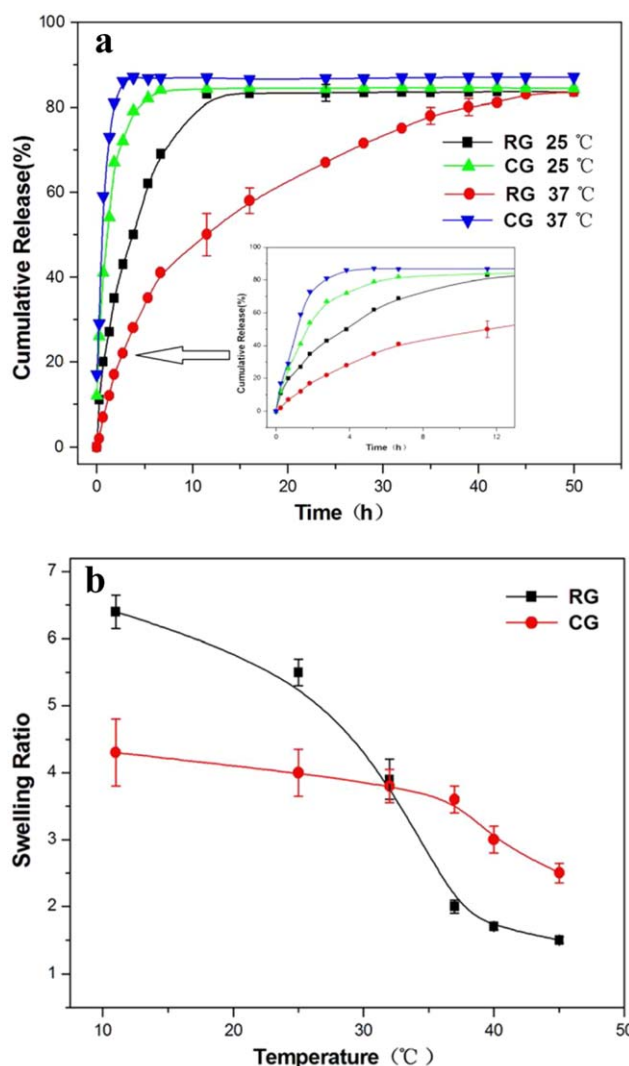


Figure 5. (a) Cumulative amounts of TCHC released from RG and CG at 25 and 37°C. The amount of drug released was determined by absorption at 357 nm with a UV spectrometer (UV-2450, Shimadzu). (b) Equilibrium SR of RG and CG over the temperature range 21–45°C. [Color figure can be viewed in the online issue, which is available at wileyonlinelibrary.com.]

the weak thermoresponsive properties of the CG, which made the gel network retained a swollen state at 37°C [Figure 5(b)] and simultaneously allowed the TCHC to move out of the hydrogel quickly, and (2) the increased temperature of the surrounding medium, which led to the increased diffusion rate of the TCHC and enhanced the release driving force.

The cumulative release of the TCHC from the RG as a function of time is illustrated in Figure 5(a). We found that the TCHC release from the RG at 37°C was significantly prolonged to 48 h; this was four times longer than that at 25°C. During the process of TCHC release from the RG, the release kinetics of the TCHC at 37°C was still determined by the swelling rate. Although RG shrunk in response to the alteration of temperature from 25 to 37°C [see Figure 5(b)], this made the gel network structure collapse drastically. The shrinkage of the gel

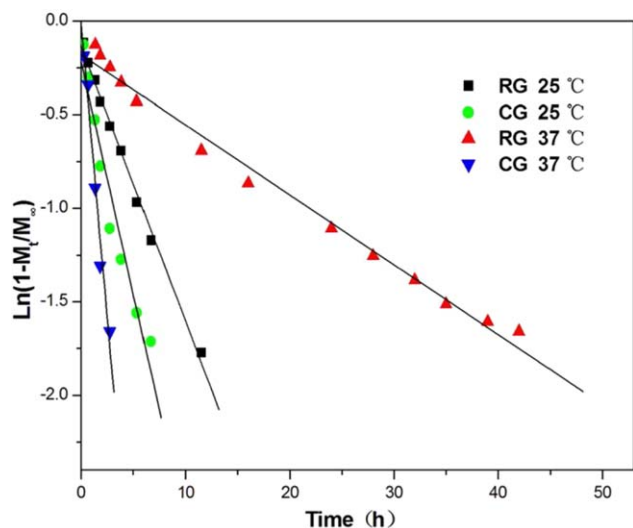


Figure 6. Plots of $\ln(1 - M_t/M_\infty)$ versus t for TCHC released from RG and CG at 25 and 37°C. [Color figure can be viewed in the online issue, which is available at wileyonlinelibrary.com.]

produced the high-density region in the surface of the hydrogel, which may have slowed the swelling rate and greatly prevented the TCHC from releasing into the medium. The slow swelling process resulted in a decrease in the diffusion rate of the TCHC in the RG and hence made the RG achieve sustained drug release at a longer period.

The simplified equation model [eq. (1)] is usually adopted to estimate the controlled release rate of the hydrogel:²¹

$$\ln\left(1 - \frac{M_t}{M_\infty}\right) = \ln\left(\frac{8}{\pi^2} - \frac{D\pi^2}{l^2}t\right) \quad (1)$$

where M_∞ is the cumulative amount of drug released at infinite time, l is the thickness of the gel disc, and D is the diffusion coefficient of the hydrogel, which could be acquired from the slope, $D\pi^2/l^2$, of the trend line by the plot of $\ln(1 - M_t/M_\infty)$ against time (t). A larger D will result in a faster drug-release rate of the gel. According to eq. (1), the fitted regression lines of the TCHC release data are shown in Figure 6, and the slope (k), D , and correlation coefficient (R^2) of the CG and RG are listed in Table I. We found that D was 0.5968 cm^2/min for the RG at 25°C, 1.0098 cm^2/min for the CG at 25°C, 0.1379 cm^2/min for the RG at 37°C, and 2.5002 cm^2/min for CG at 37°C. The

Table I. Fitting Parameters for the Release of TCHC from RG and CG at 25 and 37°C

Sample	SBMA (g)	Temperature (°C)	k (min^{-1})	D (cm^2/min)	R^2
CG	0.5	25	0.2489	1.0098	0.9493
RG	0.5	25	0.6286	0.5968	0.9942
CG	0.5	37	0.0340	2.5502	0.9756
RG	0.5	37	0.1471	0.1379	0.9845

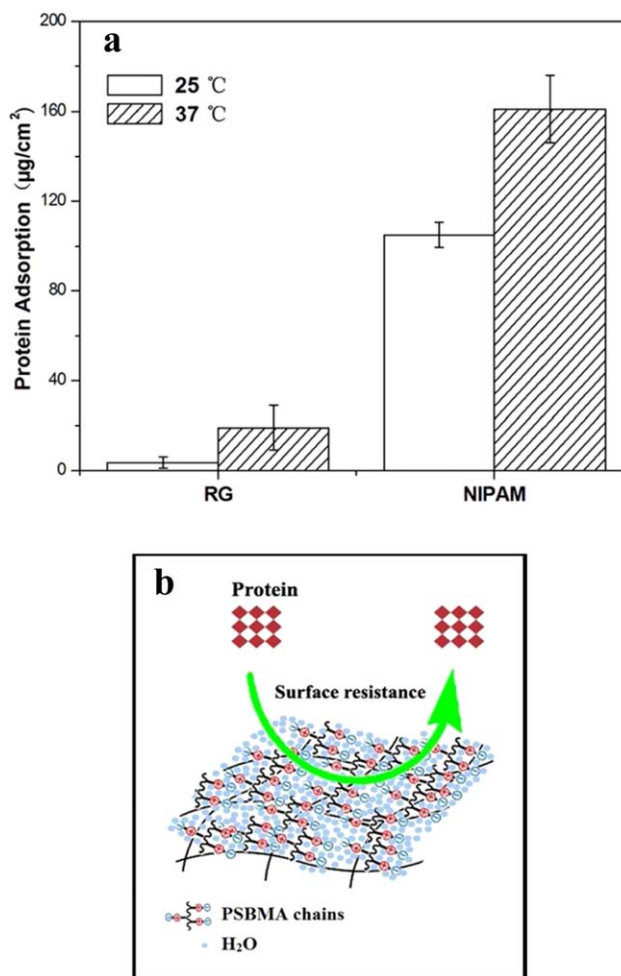


Figure 7. (a) Adsorption of RG and the PNIPAM hydrogel in a BSA solution (1.0 mg/mL) for 24 h at 25 or 37°C. (b) Illustration of the hydration of zwitterionic PSBMA chains to resist BSA adsorption on the grafted RAFT hydrogel surface. [Color figure can be viewed in the online issue, which is available at wileyonlinelibrary.com.]

smallest D for the RG at 37°C indicated RG had the slowest release rate at such temperatures; this confirmed our hypothesis that RG could achieve sustained drug release for a longer time.

Protein Adsorption Test

A Bio-Rad protein assay was carried out to evaluate the anti-protein-fouling properties of the RG and PNIPAM hydrogel at 25 and 37°C by the use of BSA as a model protein. From Figure 7(a), we observed that the BSA adsorption on the RG surface was 3.5 $\mu\text{g}/\text{cm}^2$ at 25°C and 19 $\mu\text{g}/\text{cm}^2$ at 37°C, whereas the BSA adsorption for the PNIPAM hydrogel sharply increased to 105 $\mu\text{g}/\text{cm}^2$ at 25°C and 161 $\mu\text{g}/\text{cm}^2$ at 37°C, respectively. From the BSA adsorption data, we assumed that the network structure and the medium temperature influenced the protein resistance of the gel.

In fact, the surface hydration played a critical role in the non-fouling ability of the hydrogel, whereas the strength of hydration was mainly determined by the surface packing density and chain flexibility.²² The RG could strongly resist protein adsorption because large amounts of flexible hydrophilic PSBMA

chains were grafted into the RG network; this could structurally separate from the PNIPAM backbone. Then it would bind water molecules to form a strong hydration layer near the surface via electrostatic interaction and hydrogen bonding. Such a hydration layer produced a physical barrier to prevent protein adsorption [Figure 7(b)]. However, strong surface hydration did not happen on the surface of the PNIPAM hydrogel because of the lack of the hydrophilic grafted chains in the network structure. Thus, the RG revealed market antifouling properties, whereas the PNIPAM gel did not.

The protein adsorption for both the PNIPAM hydrogel and the RG increased as the temperature rose from 25 to 37°C (Figure 7). We investigated that the enhancement in the surface hydrophobicity²³ or high surface density²² reduced the protein resistance of the gel and gave rise to more protein adsorbance on the surface. The NIPAM hydrogel was an excellently thermosensitive material, and the NIPAM structure turned from hydrophilic into hydrophobic when the temperature was higher than its phase-transition temperature (32°C). At 37°C, the NIPAM hydrogel showed hydrophobic properties; this caused more protein adsorption on the surface. For the RG, regardless of the existence of the hydrophilic grafted chains on the gel surface, it was still possible to absorb more protein on the surface because of the high surface density caused by the shrinkage of RG at 37°C.

CONCLUSIONS

The RG was successfully prepared by aqueous RAFT polymerization via PSBMA precursors with a thiocarbonylthio [—C(=S)S—R] end reaction with NIPAM. As expected, RG exhibited a fast shrinking rate in response to the temperature change and significantly decreased protein adsorption on the surface. Because of the rapid temperature-responsive properties, the RG at body temperature (37°C) could collapse, entrap drug inside the gel, and attain a long period of drug release. The structural stability, thermoresponsive and low-fouling properties, and sustained drug-release rate of the grafted RAFT gel suggested that it may have promising potential for drug-release systems.

ACKNOWLEDGMENTS

This work was financially supported by the National Science Foundation of China (contract grant sponsors 21104021 and 21176091) and the Fundamental Research Funds for the Central Universities (contract grant sponsor 20112B0006).

REFERENCES

1. Yoshida, R.; Uchida, K.; Kaneko, Y.; Sakai, K.; Kikuchi, A.; Sakurai, Y.; Okano, T. *Nature* **1995**, *374*, 240.
2. Chen, G.; Hoffman, A. S. *Nature* **1995**, *373*, 49.
3. Hoffman, A. S. *J. Controlled Release* **1987**, *6*, 297.
4. Brøndsted, H.; Kopeček, J. *Biomaterials* **1991**, *12*, 584.
5. Feil, H.; Bae, Y. H.; Feijen, J.; Kim, S. W. *J. Membr. Sci.* **1991**, *64*, 283.
6. Yoshida, R.; Takahashi, T.; Yamaguchi, T.; Ichijo, H. *J. Am. Chem. Soc.* **1996**, *118*, 5134.
7. Patil, N. S.; Dordick, J. S.; Rethwisch, D. G. *Biomaterials* **1996**, *17*, 2343.
8. Kaneko, Y.; Nakamura, S.; Sakai, K.; Aoyagi, T.; Kikuchi, A.; Sakurai, Y.; Okano, T. *Macromolecules* **1998**, *31*, 6099.
9. Ju, H. K.; Kim, S. Y.; Lee, Y. M. *Polymer* **2001**, *42*, 6851.
10. Kim, J. H.; Lee, S. B.; Kim, S. J.; Lee, Y. M. *Polymer* **2002**, *43*, 7549.
11. Liu, Q.; Zhang, P.; Lu, M. *J. Polym. Sci. Part A: Polym. Chem.* **2005**, *43*, 2615.
12. Liu, Q.; Zhang, P.; Qing, A.; Lan, Y.; Lu, M. *Polymer* **2006**, *47*, 2330.
13. Zhang, Z.; Chen, S.; Chang, Y.; Jiang, S. *J. Phys. Chem. B* **2006**, *110*, 10799.
14. Zhang, Z.; Chao, T.; Chen, S.; Jiang, S. *Langmuir* **2006**, *22*, 10072.
15. Chiang, Y.-C.; Chang, Y.; Higuchi, A.; Chen, W.-Y.; Ruaan, R.-C. *J. Membr. Sci.* **2009**, *339*, 151.
16. Xu, X.; Smith, A. E.; Kirkland, S. E.; McCormick, C. L. *Macromolecules* **2008**, *41*, 8429.
17. Yusa, S.-I.; Fukuda, K.; Yamamoto, T.; Ishihara, K.; Morishima, Y. *Biomacromolecules* **2005**, *6*, 663.
18. Wang, R.; McCormick, C. L.; Lowe, A. B. *Macromolecules* **2005**, *38*, 9518.
19. Zhang, R. *Polymer* **2005**, *46*, 2443.
20. Gürdağ, G. L.; Kurtuluş, B. *Ind. Eng. Chem. Res.* **2010**, *49*, 12675.
21. Pekcan, Ö.; Erdoğan, M. *Eur. Polym. J.* **2002**, *38*, 1105.
22. Chen, S.; Li, L.; Zhao, C.; Zheng, J. *Polymer* **2010**, *51*, 5283.
23. Herrwerth, S.; Eck, W.; Reinhardt, S.; Grunze, M. *J. Am. Chem. Soc.* **2003**, *125*, 9359.